Enhanced photoluminescence from CdS nanocrystals encapsulated by PVP and SHMP

Vikas Lahariya[1]* and Saral Kumar Gupta[2]

1. Department of Physics, Amity School of Applied Sciences, Amity University, Haryana 122413, India

2. Department of Physics, Banasthali Vidyapeeth, Rajasthan, India

The effects of the stabilizing agent on the structural and luminescence properties of cadmium sulfide (CdS) nanocrystals have been investigated. Samples were prepared by chemical precipitation method using sodium hexametaphosphate (SHMP) and polyvinyl pyrrolidone (PVP). The structural and optical properties have been studied by X-ray diffraction (XRD), ultraviolet-visible (UV-Vis) absorption, photoluminescence (PL) and Fourier transform infrared (FTIR) spectroscopy. XRD patterns confirm the presence of cubic zinc blend crystal structure with space group F-43m. The results show the variation in crystallite size with change in surfactant. Blue shift in absorption edge as compared to bulk CdS is found. PL results represent broad and very intense red emission with smaller particle size due to modification of surface emitting states with surfactant.

In the past few decades, cadmium sulfide (CdS) has been extensively studied and used for many applications. It is a well-known direct band gap semiconductor chalcogenide material, with band gap of 2.42 eV corresponding to 512 nm at room temperature with cubic face centered cubic (FCC) crystal structure[1]. It is used for light emitting diodes, solar cells, photocatalytic, optical sensors, bioimaging and optoelectronics applications[1-3]. CdS nanocrystals have higher surface reactivity due to higher surface to volume ratio and nonlinear optical properties in visible region, which are helpful for catalyst activity and fluorescence. Several methods have been used for the synthesis of CdS as nanoparticles, thin film, and core/shell nanostructures by chemical or physical methods[2-6]. In all the methods, it is essential to control the growth rate of the formation of the nanoparticles. During the nucleation and growth of particles, initially formed seeds grow, over the time, in size in a thermodynamically controlled manner to form primary particles. If this growth of particles is not controlled, due to Ostwald ripening and van der Waals interactions between particles, they will agglomerate and settle down[6]. The agglomeration can be arrested by either stabilizer or capping agent and by controlling the reaction. To date, lots of methods have been developed to stabilize the surfaces of the nanoparticles with organic or inorganic groups against agglomeration[7]. However, kinetic growth, surface stability and relaxation dynamics of electronic states at nanoscale have been the subject of interest. Suitable capping agent prevents agglomeration by encapsulation and

modifies shape stability and some optical properties of the nanoparticles. For this work, some polymeric stabilizing agent, such as polyethylene glycol (PEG) methacrylic acid (MA)[8], poly vinyl alcohol (PVA)[2], sodium hexametaphosphate (SHMP)[9] and polyvinyl pyrrolidone (PVP), have been widely used for metal oxide and metal sulfide nanoparticles[10-12]. They provide high surface stability, and significantly influence the structural, morphological, and optical properties of nanoparticles[10,11]. Previous studies on PVP capped metal or semiconductor nanoparticles have been carried out[10-12]. The studies demonstrated that the PVP effectively restricts the Ostwald ripening kinetics growth rate of semiconductor nanoparticles[11,12]. Our previous study on PVP capped Mn doped ZnS nanoparticles also expressed the role of PVP on size related luminescence properties[13]. Apart from it, SHMP has also been widely used as surfactant for synthesis of oxide nanomaterials[9]. It has good dispersion and adhesion properties. To the best of our knowledge, there are very few reports available on optical properties of chalcogenide semiconductor with SHMP as a surfactant[14,15]. Among them, most of the studies were focused on the dopant nature. In this connection, we reported the comparative study on structural and luminescence properties of CdS nanoparticles prepared using PVP and SHMP as stabilizing agent. PVP polymer and SHMP are water soluble, and they can interact with the metal ions by complex or ion-pair formation and can be used to design certain physical properties of semiconductor nanoparticles[11]. The present work provides an insight to

realize the passivation effects of PVP/SHMP surfactant on the structural and optical properties of CdS nanoparticles.

All the reagents were analytical grade (AR) and used without any further purification. The CdS nanoparticles are synthesized by chemical precipitation method using PVP and SHMP as stabilizing agents, cadmium acetate and sodium sulfide ($Na_2S \cdot 2H_2O$) (Merck India) are used as cadmium and sulfur source, respectively. The synthetic method for CdS nanoparticles applied in this work is as follows.

The synthesis reaction is carried in the aqueous medium at air atmosphere. Solutions of 5.761 7 g $Cd(CH_3COO)_2$, 1.952 5 g Na_2S and 0.5 g PVP are prepared in 50 mL de-ionized water separately. First, the PVP solution is added with $Cd(CH_3COO)_2$ solution by stirring continuously. Next, 50 mL of Na_2S solution is added to the above solution slowly with constant stirring. The pale-yellow color precipitate is collected from the solution. To remove the un-soluble impurities, the sample is washed many times using de-ionized water and acetone alternatively. The washed sample is dried at 40 °C in air for 1 h. For the synthesis of SHMP-capped CdS nanoparticles, SHMP is used instead of PVP with the same precursor composition. The samples are characterized by X-ray diffraction (XRD) ranging from 20° to 80° with step size of 0.2°. The transmission electron microscope (TEM) images are collected from Technai 2G^2 instrument. The ultraviolet-visible (UV-Vis) absorption spectrum is recorded by Perkin Elmer λ-25 spectrometer, and photoluminescence (PL) spectra are carried out by the Fluromax-3 spectrometer over the wavelength range from 450 nm to 800 nm. The Fourier transform infrared (FTIR) spectroscopy is recorded on a Bruker AlphaT spectrometer. Here the sample is used in the powder form for analysis.

In the proposed mechanism, synthesis of CdS nanoparticles is similar to that suggested by WARAD et al for ZnS nanoparticles[15]. Cadmium acetate dissociates into cadmium ions (Cd^{2+}) and acetate (Ac^-) ions in aqueous medium. Similarly, Na_2S dissociates into its respective cations and anions. Since Na^{2+} is more reactive than Cd^{2+}, readily Na_2(acetate) can be formed. After the Cd^{2+} and S^{2-} reaction, CdS nucleates have been subsequently grown in the solution by consuming more and more ions from it. During the nucleation and growth process, by employing PVP and SHMP layer over the nanoparticles, it induces a repulsive force between the nanoparticles and impedes aggregation of particles. Hence, the steric hindrance effect of larger molecules or polymers helps to avoid agglomeration. Further, the structural and optical investigations confirm the formation and encapsulation of CdS nanoparticles. XRD patterns of the CdS-PVP and CdS-SHMP samples are shown in Fig.1.

The three diffraction peaks corresponding to reflections from (1 1 1), (2 2 0), and (3 1 1) planes of the cubic (zinc blend) phase [JCPDS 89-0440] with space group

(F-43m) are obtained. However, (111) peak of cubic phase is more likely to (002) peak of hexagonal structure although no other peak of hexagonal structure was found. Thus, structure is predominately cubic. No impurity peak found indicates the single-phase formation of the samples. However, the broadening of the most prominent peak (111) indicates the nanocrystalline nature of the samples. The average crystallite size is calculated using the Debye-Scherrer formula[1] as

$$D = k\lambda/\beta\cos\theta, \tag{1}$$

where k is a geometric factor of 0.9, λ is the X-ray wavelength of 1.546 Å, β is the full width at half maximum (*FWHM*) of diffraction peak, and θ is the diffraction angle. The calculated crystallin size is 5.95 nm for CdS, 4.58 nm for CdS PVP and 3.29 nm for CdS SHMP. The calculated crystallite size is found to be smaller for SHMP encapsulated CdS nanoparticles. The reduction of particle size indicates the pronounced effect of the stabilizer on the surface of nanoparticles in aqueous medium. The peaks are slightly shifted to lower angle, which might be due to the presence of small tensile strain in the sample. The residual stress originates from dislocations, and grain boundaries appear in the samples[13]. Moreover, the decrease in peak intensity with the SHMP/PVP indicates the decrease in crystallinity. The degree of crystallinity is calculated by $N_c = (I_c - I)/I$, where I_c represents the intensity of SHMP capped CdS and I represents the intensity of PVP capped CdS sample. The negative value of N_c indicates less crystalline samples with SHMP surfactant. The calculated lattice constant and inter planner spacing using Bragg's formula are 5.77, 5.78 and 5.81 for CdS, CdS PVP and CdS SHMP samples, respectively.
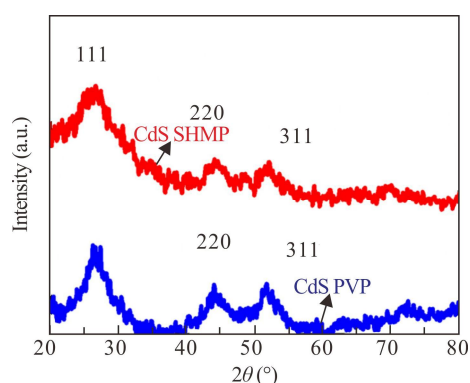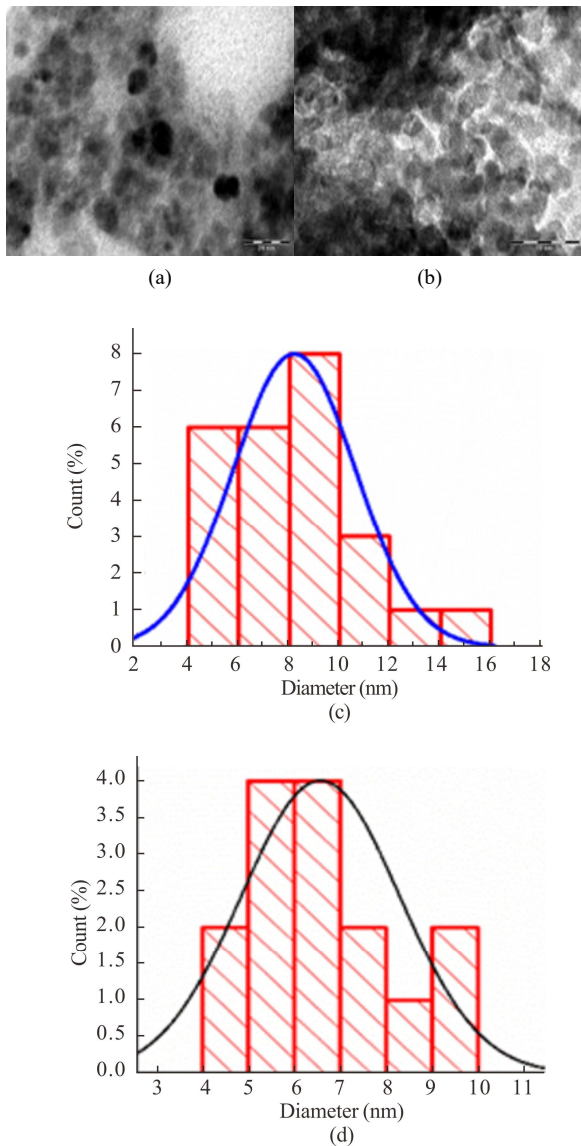

Fig.1 XRD pattern of CdS nanocrystals

Furthermore, no major effect on structural parameters reveals that the surfactant only encapsulated the surface of CdS nanoparticles by physical adsorption on the surface[14]. This is achieved by the absorbing a layer of PVP/SHMP over the nanoparticle inducing steric hindrance by employing the PVP and SHMP. The steric stabilization effect is induced by adsorption of surfactant on the surface of particles. Thus, the osmatic repulsion

between the approaching particles consequently restricts the particles growth. In addition, steric stabilization has advantage over electrostatic stabilization that it can be achieved in aqueous media. Therefore, high solubility in water also helps to promote the stabilizing chain strongly adsorbed over the surface of nanoparticles. It has been achieved by the adsorption of PVP/SHMP molecules onto the surface of the CdS to encapsulate the nanoparticles by inducing steric hindrances at appropriate stages in the precipitation reaction. The TEM images (Fig.2) of PVP/SHMP capped CdS nanoparticles show the formation of nearly spherical shape with broad size distribution in the range of 2—12 nm. Further, the images indicate that the CdS nanoparticles are well dispersed and uniformly distributed in the medium, with estimated sizes of 6.5 nm and 8 nm for SHMP capped CdS and PVP capped CdS samples, respectively.

(a)   (b)

(c)

(d)

Fig.2 (a) TEM image and (c) histogram of CdS PVP nanocrystals; (b) TEM image and (d) histogram of CdS SHMP nanocrystals

The absorption spectra of CdS nanoparticles are shown in Fig.3. The SHMP capped CdS nanoparticles exhibit an absorption edge at 474 nm and PVP capped CdS at 483 nm. They are considerably blue-shifted relative to the absorption edge of uncapped CdS sample (512 nm), indicating increased effective energy band gap due to quantum size effect. In addition, it can be observed that intense absorption towards shorter wavelength is high with encapsulated CdS nanoparticles due to higher electronic state transition. In case of uncapped CdS, excitonic structure is not found, while capped CdS exhibits exciton absorption peak at 428 nm due to 1S-1S* absorption. The presence of exciton absorption band may be attributed to exciton binding energy. The effective energy band gap is calculated from Tauc relation as
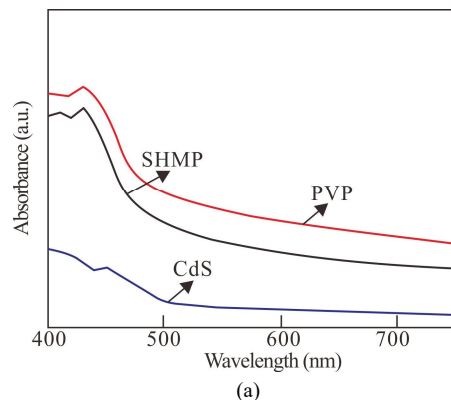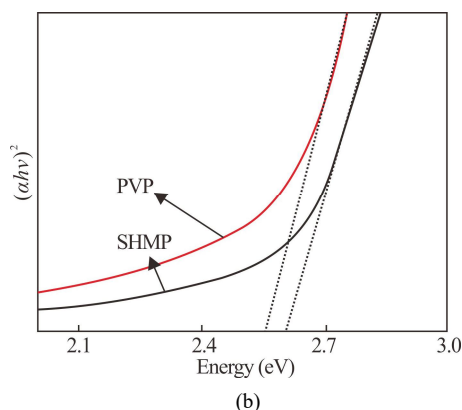
$$(\alpha h v)^{1/n} = A(h v - E_g), \tag{2}$$

where α is absorption coefficient, hv is incident photon energy, and E_g is the effective band gap. For direct band gap CdS, $n=1/2$, so extrapolating the straight line of $(\alpha h v)^2$ on X axis is used to estimate the effective band gap[16]. The calculated band gap is 2.61 eV and 2.56 eV for SHMP-CdS and PVP-CdS respectively larger than bulk CdS. The widening of effective energy band gap with PVP and SHMP stabilizing agent can be explained in term of better particle size distribution and formation of smaller particles with SHMP. The size of the nanoparticles is calculated by Brus equation based on effective mass approximation (EMA) model[10] as

$$E_{gn} = E_{gb} + 2.599/R^2 - 0.303 \, 1/R. \tag{3}$$

The calculated size by XRD is smaller as compared to estimated size by EMA, which might be attributed to over estimation of the EMA method. Thus, estimated size by considering effective energy band gap is found to be larger than real crystal size[17].

The exciton Bohr radius for CdS is about 30 Å[16]. According to the reported work, when the radius of CdS satisfies $R/\alpha_B < 4$, the motion state of the lowest level is due to the individual particle confinement region[12,16]. The results are consistent with those in Refs.[2, 12].
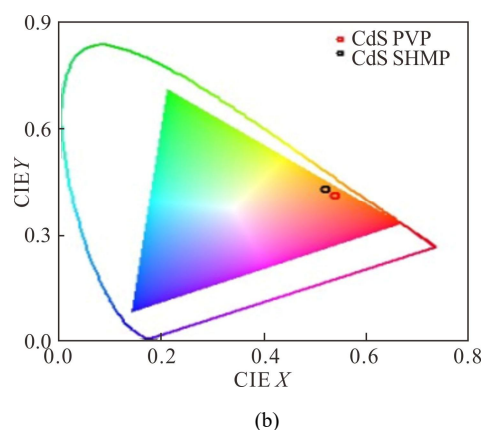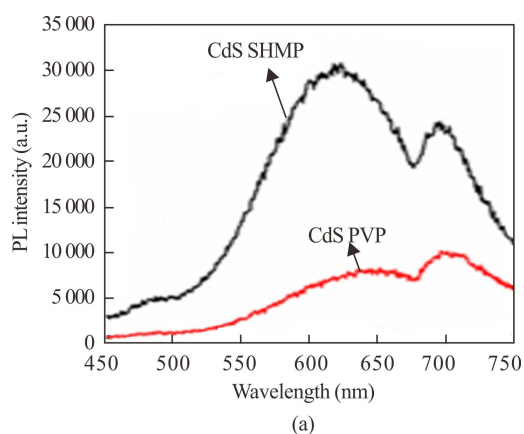

(a)

(b)

Fig.3 (a) Absorption spectra and (b) Tauc plot curves of CdS nanocrystals (CdS PVP and CdS SHMP)

The PL spectra of PVP and SHMP encapsulated CdS nanoparticles at room temperature are shown in Fig.4(a). The PL is excited by 425 nm. Band edge luminescence is not found, although a broad red emission has been observed. The inhomogeneous broadening in red emission band indicates the presence of multiple bands of short wavelength in the spectrum. Therefore, with the deconvolution of PL band, two emission peaks could be observed in all the PL spectrum. The observed PL peak positions are 612 nm and 706 nm for CdS-PVP (Fig.4(c)) and 618 nm and 712 nm for CdS-SHMP nanocrystalline samples (Fig.4(d)). It is found that the PL peak 1 is the most intense and relatively broad for SHMP capped CdS nanoparticles, while the second peak intensity is higher for PVP capped CdS nanoparticles. Hence, the PL peak position and intensity are slightly changed with the change in the surfactant. However, the PL spectrum of CdS-SHMP is much intense as compared to that of CdS-PVP nanoparticles. In general, defects related emission is produced by the transition or recombination of electrons from the trap or donor states to the valence band. Such donor states are formed from sulfur vacancy and transition to the valence band, resulting in the red emission[18]. Moreover, it is reported that Na_2S chalcogenide source can provide much more sulfide ions[15]. Therefore, excess sulfide may create surface defects at the interface, and radiative recombination from these trap states leads to emission at higher wavelengths. Previous results also observed the effect of a chalcogenide source on the PL[15,19]. Similar results were reported by WAGEH et al using sodium sulfide and thiourea as different sulfide ion sources for ZnS nanocrystals[19]. The main objective of the surfactant is to provide electronic surface passivation of weak dangling bonds. The significant increase in intensity of PL emission indicates that surfactant eliminates the surface trap caused by dangling bonds. Furthermore, the PL peak I becomes broader with SHMP surfactant. It is due to wider particle size distribution, which was confirmed by TEM measurement. The size dependent shift of defects related emission arises from the recombination of electrons at mid
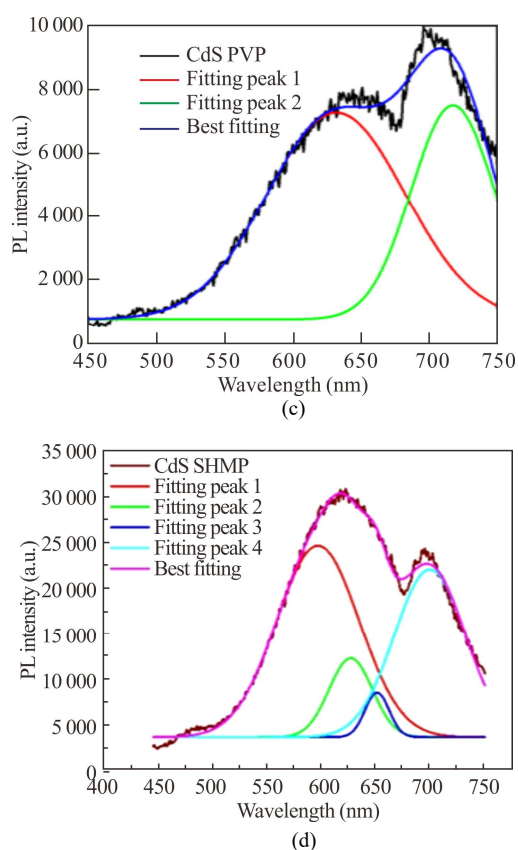
gap states, as the electrons at trap states still possess small effective mass[16]. Since the relaxation dynamics depends on the chemical modification of surface of nanocrystals, different relaxation processes may occur with different surfactants[12]. In addition, different relaxation pathways for charge carrier recombination formed during the excitation[20]. Hence the change in the surface emitting states and complex interaction between stabilizing agent and CdS consequently modify the intensity of the defects related emission. Previous PL results on PVP capped CdS by SADHU et al[12] discussed the bonding of complexation of Cd with the lone pair of nitrogen. Pyridine is known to act as a hole acceptor and hole transfer to adsorbed pyridine ligands, and therefore quenches any transition associated with the hole. Fig.4(b) represents the CIE 1931 color coordinates for PL of CdS-PVP and CdS-SHMP nanoparticles. Calculated values of CIE coordinates are (0.52, 0.43) for CdS-SHMP and (0.54, 0.41) for CdS-PVP, appearing as red color emission. The color correlated temperature (CCT) specifically determines the proximity of the emitted radiation. It is estimated by using Mc-Camy empirical formula[21] as

$$CCT = -437n^3 + 3\ 601n^2 - 6\ 861n + 5\ 514.32, \qquad (4)$$

where $n=(x-x_e)/(y-y_e)$, $x_e=0.332\ 0$, $y_e=0.185\ 8$. The estimated value is about 2 000 K and less than 5 000 K, suggesting warm light used for domestic light applications.
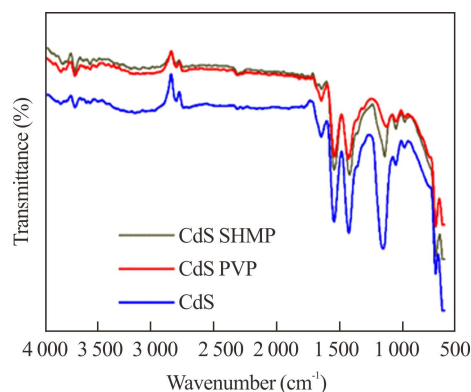

(a)

(b)

(c)

(d)

Fig.4 (a) PL spectra of CdS nanocrystals; (b) CIE diagram; Deconvoluted PL spectra of (c) CdS PVP and (d) CdS SHMP

Fig.5 shows the FTIR spectra of PVP and SHMP encapsulated CdS nanoparticles. The different IR bands in the spectrum provide the information about the bonds and their nature. In PVP, C=O, C-N and CH_2 functional groups are presented. A polar amide group within the pyrrolidone ring and its hydrophobic carbon chain helps to prevent aggregation of nanoparticles by steric hinderance effect[22]. On the other hand, the main ingredient of biocompatible SHMP is hydrogen phosphate ($H_2PO_4^-$), which absorbs on the surface of metal ions via electrostatic force[23]. The IR peaks appear in the lower wavenumbers of 652 cm^{-1} and 675 cm^{-1} in fingerprint region due to Cd-S vibrations in PVP and SHMP capped CdS nanoparticles. The absorption at 1 108 cm^{-1} is attributed to the presence of alkoxy C-O in all the samples. In the preparation of CdS, $Cd(CH_3COO)_2$ is used, so intense C-O stretching modes at 1 500—1 650 cm^{-1} and at 2 360 cm^{-1} are due to the oxygen stretching modes arising from adsorption of CO_2 on the surface of nanoparticles[24]. The peaks at 1 407 cm^{-1} and 2 881 cm^{-1} correspond to C-H bonding, which is attributed to the formation of coordinate bond between nitrogen atom and Cd^{2+} ions. A weak blue shifted peak at 1 742 cm^{-1} is observed due to carboxylic group in PVP capped CdS. A dangling interaction occurred only due to dipole interaction between O of C=O and CdS. The 1 646 cm^{-1} indicates the hygroscopic nature of PVP. The presence of

OH group indicates the existence of water absorbed in the surface of nanocrystals. In case of SHMP capped CdS nanocrystals, narrow peaks found at 1 648 cm^{-1} and 913 cm^{-1} indicate nitrogen-oxygen interaction. The presence of the band 1 097 cm^{-1} ensures phosphorous-oxygen interaction of SHMP to CdS. Thus, SHMP will prevent the growth of particles by steric stabilization. In case of capped CdS samples, no new peak can be observed, but the position and intensity of the peaks are slightly changed, due to the interaction with CdS. The results agree with Ref.[15]. Furthermore, the peaks become considerably weakened with PVP and SHMP surfactant.

Fig.5 FTIR spectra of CdS nanocrystals

In summary, the effect of the stabilizing agent PVP and SHMP on the structural and optical properties of CdS nanoparticles has been investigated. The results reveal that SHMP is more effective compared to PVP, and it exhibits smaller size and larger energy band gap with higher transmittance. Enhanced luminescence with red emission band has been obtained with SHMP capped CdS nanoparticles. The passivation effect on surface defects by surfactant PVP/SHMP is analyzed. The interaction between CdS and phosphate ions of SHMP can modify the size and optical characteristics of CdS nanoparticles. Depending on the surfactant chemical nature, the growing CdS nanoparticles are stabilized by the surfactants to different extents. The study may be helpful for analyzing the CdS nanocrystals for potential applications in optoelectronic devices and fluorescence applications.

Statements and Declarations

The authors declare that there are no conflicts of interest related to this article.

References

[1]　DONGRE J K, NOGRIYA V, RAMRAKHIANI M. Structural, optical and photoelectrochemical characterization of CdS nanowire synthesized by chemical bath deposition and wet chemical etching[J]. Applied surface

science, 2009, 255(12)：6115-6120.

[2]   LAHARIYA V. Study of electroluminescence in cadmium sulfide polymer nanocomposite films[J]. Journal of nano research, 2017, 49：181-189.

[3]   BANERJEE R, JAYAKRISHNAN R, AYYUB P. Effect of the size-induced structural transformation on the band gap in CdS nanoparticles[J]. Journal of physics：condensed matter, 2000, 12(50)：10647-10652.

[4]   NOGRIYA V, DONGRE J K, RAMRAKHIANI M, et al. Electro-and photo-luminescence studies of CdS nanocrystals prepared by organometallic precursor[J]. Chalcogenide letters, 2008, 5(12)：365-373.

[5]   LAHARIYA V, KUMARI E, SINGH N. Optical investigation of starch capped cadmium sulfide nanoparticles[J]. Materials today：proceedings, 2022, 48(3)：622-625.

[6]   MALLIK K, MANDAL M, PRADHAN N, et al. Seed mediated formation of bimetallic nanoparticles by UV irradiation：a photochemical approach for the preparation of core-shell type structures[J]. Nano letters, 2001, 1(6)：319-322.

[7]   CELEBI S, ERDAMAR A K, SENNAROGLU A, et al. Synthesis and characterization of poly (acrylic acid) stabilized cadmium sulfide quantum dots[J]. Journal of physical chemistry B, 2007, 111：12668-12675.

[8]   DEVI J, DUTTA P. A study on dielectric properties of cadmium-zinc sulphide core-shell nanocomposites for application as nanoelectronics filter component in microwave domain[J]. Journal of electronic materials, 2018, 47(7): 3529-3542.

[9]   SUTHAKARAN S, DHANAPANDIAN S, KRISH-NAKUMAR N, et al. Hydrothermal synthesis of surfactant assisted Zn doped SnO$_2$ nanoparticles with enhanced photocatalytic performance and energy storage performance[J]. Journal of physics and chemistry of solids, 2020, 141：109407.

[10]   LAHARIYA V, RAMRAKHIANI M. Luminescence study on Mn, Ni co-doped zinc sulfide nanocrystals[J]. Luminescence, 2020, 35(6)：924-933.

[11]   AMMA B S, RAMAKRISHNA K, PATTABI M. Comparison of various organic stabilizers as capping agents for CdS nanoparticles synthesis[J]. Journal of materials science：materials in electronics, 2007, 18(11)：1109-1113.

[12]   SADHU S, CHOWDHURY P S, PATRA A. Synthesis, and time-resolved photoluminescence spectroscopy of capped CdS nanocrystals[J]. Journal of luminescence,

2008, 128(7)：1235-1240.

[13]   LAHARIYA V, KUMAR S. Study on structural and optical properties of Sb$_2$S$_3$ and CdI$_2$ composite thin films deposited by thermal vapor deposition[J]. International journal of nanoscience, 2018, 17(04)：1760033.

[14]   MURUGADOSS G. Synthesis and optical characterization of PVP and SHMP-encapsulated Mn^{2+}-doped ZnS nanocrystals[J]. Journal of luminescence, 2010, 130(11)：2207-2214.

[15]   WARAD H C, GHOSH S C, HEMTANON B, et al. Luminescent nanoparticles of Mn doped ZnS passivated with sodium hexametaphosphate[J]. Science and technology of advanced materials, 2005, 6(3-4)：296-301.

[16]   THAKUR S, DAS P, MANDAL S K. Solvent-induced diversification of CdS nanostructures for photocatalytic degradation of methylene blue[J]. ACS applied nano materials, 2020, 3(6)：5645-5655.

[17]   MARANDI M, TAGHAVINIA N, MAHDAVI S M. A photochemical method for controlling the size of CdS nanoparticles[J]. Nanotechnology, 2005, 16 (2)：334.

[18]   LOZADA-MORALES R, ZELAYA-ANGEL O, TORRES-DELGADO G. Photoluminescence in cubic and hexagonal CdS films[J]. Applied surface science, 2001, 175：562-566.

[19]   WAGEH S, SHU-MAN L, YOU F T, et al. Optical properties of strongly luminescing mercaptoactic-acid-capped ZnS nanoparticles[J]. Journal of luminescence, 2003, 102：768-773.

[20]   KUMAR S, GRADZIELSKI M, MEHTA S K. The critical role of surfactants towards CdS nanoparticles：synthesis, stability, optical and PL emission properties[J]. RSC advances, 2013, 3(8)：2662-2676.

[21]   MCCAMY C S. Correlated color temperature as an explicit function of chromaticity coordinates[J]. Color research & application, 1992, 17(2)：142-144.

[22]   KOCZKUR K M, MOURDIKOUDIS S, POLAVARAPU L, et al. Polyvinylpyrrolidone (PVP) in nanoparticle synthesis[J]. Dalton transactions, 2015, 44(41)：17883-17905.

[23]   LU J, SUN M, YUAN Z, et al. Innovative insight for sodium hexametaphosphate interaction with serpentine[J]. Colloids and surfaces A：physicochemical and engineering aspects, 2019, 560：35-41.

[24]   LI Z H, HAN Y X, LI Y J, et al. Effect of serpentine and sodium hexametaphosphate on ascharite flotation[J]. Transactions of nonferrous metals society of China, 2017, 27(8)：1841-1848.